



Survey of deep tail plasma sheet crossings: plasma sheet distributions resulting from reconnection

R. T. Mist, C. J. Owen

Mullard Space Science Laboratory, University College London, UK

T. Mukai

Institute of Space and Astronautical Science (ISAS), Sagamihara, Kanagawa, Japan

Abstract. We illustrate the structure of the distant ($X < -60 R_e$) plasma sheet and separatrix layers in terms of low energy ion distributions observed by Geotail. In a statistical survey, ion distributions are classified as single or multi-component. Multi-component populations are clearly observed in 68 % of tailward flows. In two crossings only multi-component populations are observed and in two crossings no multi-component populations are identified. Although multi-component plasmas occur throughout the plasma sheet, they are observed more often in the outer region. Previous plasma sheet formation models do not predict multi-component distributions in the centre of the plasma sheet. However, this data supports the *Owen and Mist* [2001] model that predicts a similar plasma sheet structure.

Introduction

In early MHD models of distant tail reconnection, plasma acceleration occurs at slow shocks bounding the plasma sheet. Assuming all the acceleration takes place at the shocks, they should represent a clear boundary between lobe and plasma sheet particle distributions. Although *Nagai et al.* [1998] observed near-isotropic plasma in the near-Earth plasma sheet, the data in the distant tail are not generally consistent with this [*Hoshino et al.*, 2000]. Large scale hybrid simulations of magnetotail reconnection suggest a more complex plasma sheet and plasma sheet boundary layer (PSBL) structure [*Krauss-Varban and Omidi*, 1995; *Lin and Swift*, 1996]. These models identify multi-component populations in the PSBL (or separatrix layer) and also in a region upstream of the shocks. In the central plasma sheet, near isotropic (i.e. single temperature Maxwellian) distributions are predicted.

Ion distributions observed during rapid distant crossings of the plasma sheet will be compared with predictions from two recent plasma sheet formation models [*Hoshino et al.*, 2000; *Owen and Mist*, 2001]. *Hoshino et al.* [2000] present 2 case studies in which they identify 2 distinct plasma sheet regions; an outer region containing anisotropic plasma distributions, and an inner region, closer to the current sheet, which they claim contains isotropic plasma. In the outer region, a slow-flowing, cold, lobe-like population and a heated, accelerated, lima bean-shaped population were observed.

The *Hoshino et al.* model has 2 slow shocks at the edge of the outer plasma sheet. Within these, the authors suggest a tangential discontinuity pair marks the limits of the isotropic region. However, the case studies presented are not clearly consistent with ion acceleration taking place solely at the slow shocks. While some distributions support this description, *Hoshino et al.* also show inner region ion distributions that are clearly anisotropic. These have a shell-like structure superposed on a lima-bean population. Moreover, only 20% of lobe/plasma sheet boundaries could be positively identified as slow shocks [*Saito et al.*, 1995].

Various plasma sheet models have been suggested in which acceleration and heating take place along the length of the magnetotail at a central current sheet threaded by hairpin field lines [*Cowley*, 1980; *Owen et al.*, 1991; *Owen and Mist*, 2001]. The structure of the plasma distributions is determined by balancing field and particle stresses at the current sheet. A lobe-like population and various accelerated populations should be seen simultaneously across the plasma sheet. *Owen and Mist* [2001] also postulate that some outflow ions are backscattered, possibly due to small scale structures and waves observed in this region [*Nishida et al.*, 1998]. The backscattered ions may undergo Fermi acceleration and hence form a shell of high energy ions in addition to the inflow and lima bean populations. *Owen and Mist* suggest the scattering process is probably stronger adjacent to the central current sheet. Thus there will be an inner plasma sheet containing the cold inflow, lima bean and a full shell of energetic ions. The energetic ions provide pressure and support this region's weak field. These distributions may also be isotropic. Next to this, an outer region contains cold inflow ions and outflow ions able to escape the inner plasma sheet; the lima bean and high energy hemispherical shell populations. Beyond the outer plasma sheet, but in the PSBL, only multiply reflected high energy ions and the inflow population are predicted.

In this paper, we conduct a survey of deep tail plasma sheet crossings made by Geotail. The proportion of distributions in which multiple rather than single component populations are clearly observed is determined. The observed field strength is used to indicate Geotail's proximity to the central current sheet and thus obtain an indication of the spatial structure across the region.

Data Analysis

We identified rapid complete plasma sheet crossings in 3 Geotail deep tail orbits between April 4 and October 13, 1994. Restricting the data set to rapid crossings (< 15 min)

Copyright 2001 by the American Geophysical Union.

Paper number 2001GL013396.
0094-8276/01/2001GL013396\$05.00

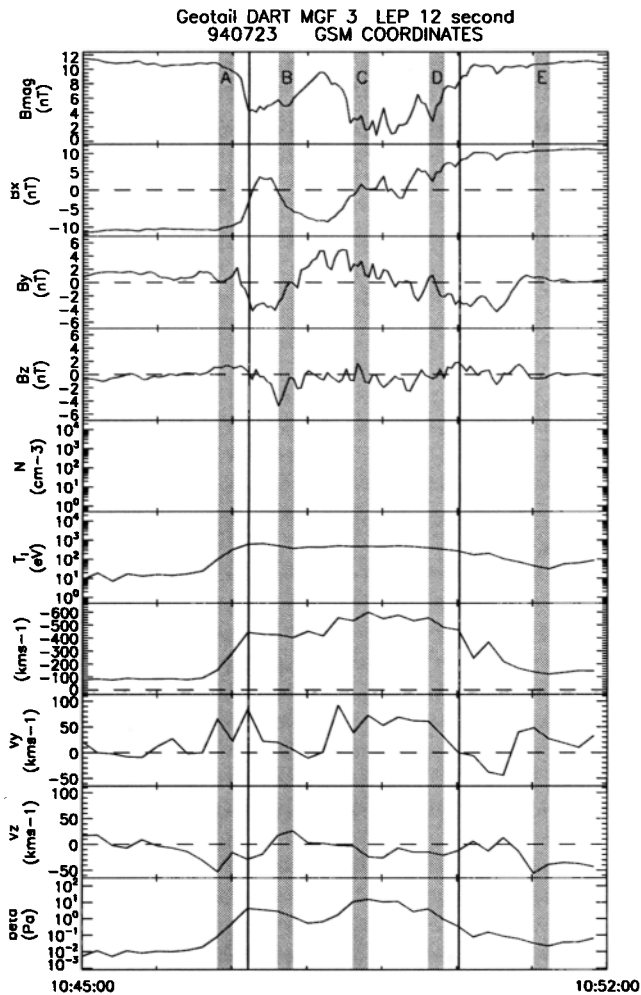


Figure 1. July 23, 1994: Magnetic field and plasma moment data from Geotail. The vertical black lines indicate that boundaries of the region containing distributions identified as plasma sheet. The grey bars show the time periods during which the 12 s distributions displayed in Figure 2 were obtained.

minimised temporal variations caused by solar wind fluctuations. 33 such crossings were observed, lasting for a combined 3.2 hrs (958 12 s 2D plasma distributions from the LEP instrument [Mukai *et al.*, 1994]). In order to study the simplest reconnection geometry, this analysis is restricted to observations of tailward flowing plasma. These are assumed to be tailward of a reconnection region and, unlike near-Earth observations, free from complications associated with particle mirroring and tailward pressure gradients. The data set contains 843 tailward flowing plasma distributions.

We use the magnetic field magnitude to give an indication of Geotail's proximity to the central current sheet. The direction of the X_{GSE} component indicates whether Geotail is north (+) or south (-) of the cross tail current sheet. In the PSBL, $|B|$ decreases slightly from lobe values. In the plasma sheet $|B|$ is observed to decrease and reach ~ 0 at the centre before increasing again after B_x changes sign.

Case Study

Figure 1 shows a rapid plasma sheet crossing between 10:45 and 10:52 UT on July 23, 1994. Geotail was located at $(-135, -5, 0.5) R_e$ (GSM). The figure shows 3 s resolution data from the MGF instrument [Kokubun *et al.*, 1994], and 12 s resolution LEP moment data. The top 4 panels show the magnitude and components of the magnetic field (nT). Panels 5 and 6 show ion density (cm^{-3}) and ion temperature (eV). The next 3 panels show the ion velocity components (km s^{-1}). The bottom panel shows plasma beta (β). The black vertical lines indicate the limits of the region containing plasma sheet ion distributions included in this survey. In this period there are 15 individual distributions.

During this period Geotail crossed the plasma sheet from south to north in about 2.5 min. In the lobes, $|\vec{B}| \sim 11$ nT, and drops to 5 nT in the plasma sheet with a minimum of 2 nT. The ion temperature increases from 20-70 eV in the lobes to 450 eV in the plasma sheet. The lobe density is 0.2 cm^{-3} and the plasma sheet density is 0.4 cm^{-3} . The bulk velocity in the lobes -120 km s^{-1} . In the plasma sheet it averages -500 km s^{-1} , reaching -600 km s^{-1} at times. This is consistent with reconnection models, which typically predict that the flow speed should be of order the lobe Alfvén speed ($\sim 540 \text{ km s}^{-1}$). We note that, as expected, β is enhanced in the plasma sheet compared with both the lobe and PSBL.

Figures 2a-e show five 2D ion distributions observed during this period. The vertical grey bars marked A-E in Figure 1 indicate when these 12 s distributions were taken. The left hand side of each figure contains the 2D data, showing the phase space density (PSD) in each energy bin along each of the 16 sectors. Sector 14 contains particles moving roughly in the tailward direction and sector 10 contains particles moving in the duskward direction. The colour scale indicates the logarithm of PSD. The red traces on the right show the PSD of the sector containing an apparent axis of symmetry of the distributions (highlighted red). The black trace is the one count level of the instrument, data below this have been excluded. The orange region under the red trace contains the lowest energy channels, corresponding to the energies observed in the lobes.

Figures 2a and 2e contain data taken by Geotail in the PSBL ($|B| = 10.3$ and 9.2 nT respectively). The inflowing lobe population is clearly visible near the centre of the plot. A separate population of tailward-flowing, high-energy particles is also evident. In the plasma sheet proper, we see a variety of distributions. Figures 2b and 2d contain multi-component populations ($|B| = 5.1$ and 4.2 nT respectively). At low energies a cold, slow-flowing population, similar to those observed in the adjacent PSBL, is clearly visible. Also, a heated, accelerated population is observed moving faster than the inflow and directed along sector 13. These heated populations show a lima bean-shaped structure, particularly in Figure 2d where this feature is clearly picked out by the contouring. In Figure 2b, it is not so clear but the trace through the distribution (right panel) shows at least two clear populations. In Figure 2b and 2d, higher energy shell similar to those observed in the PSBL is also evident at velocities above those of the lima bean population. In Figure 2b particularly, these particles are also seen moving Earthward. Finally, Figure 2c contains data recorded when $|B| = 2.8$ nT, suggesting Geotail was most likely located closer to the central current sheet. In this distribution we were not

able to clearly identify more than a single ion population. For further examples of these types of distributions we refer the reader to *Hoshino et al.* [2000].

Statistical analysis

The above case study illustrates the variety of ion distributions observed in and around the distant reconnection plasma sheet. We now examine whether the centre of the plasma sheet consistently exhibits an ‘isotropic’ or single component plasma, as predicted by the slow shock

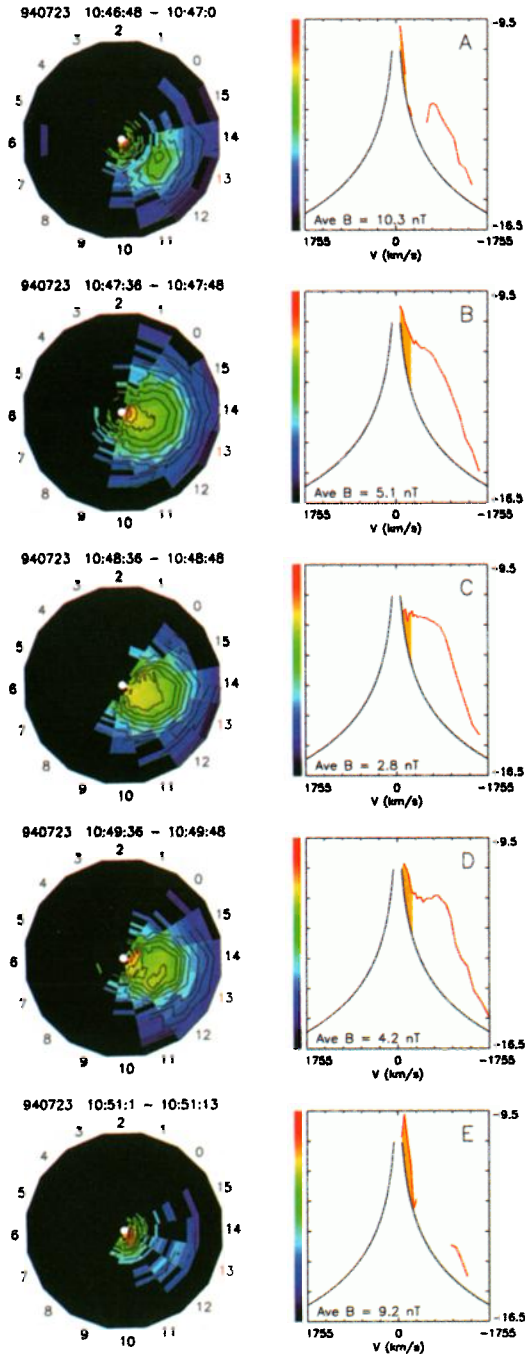


Figure 2. These 2D ion distributions show the plasma populations in the PSBL (2a, 2e) and the inner (2c) and outer plasma sheet (2b, 2d).

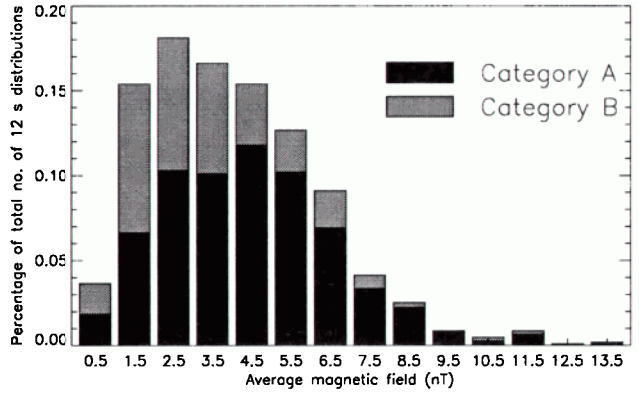


Figure 3. The percentage of the total data base which are category A (black) and category B (grey) distributions, ordered with respect to $|\bar{B}|$.

and tangential discontinuity models [*Hoshino et al.*, 2000] or whether multiple components are observed across the entire plasma sheet as in the current sheet acceleration model [*Owen and Mist*, 2001]. To do this, the ion distributions obtained during these three deep tail crossings were split into two, visually identified, categories; (A) the observed distribution clearly contains two or more components; (B) the distribution does not contain two clear components. The ordered data are then used to examine the plasma sheet structure normal to the current sheet, tailward of a reconnection region. Note that *Hoshino et al.* [2000] concluded on the basis of two case studies that category (A) distributions occur in the outer plasma sheet and category (B) distributions occur in the inner plasma sheet.

In Figure 3, we display the survey results, ordered with respect to average plasma sheet field magnitude. The chart shows the fraction of the database classified as Category A (black) and Category B (grey). Considering tailward flow events, 576 clearly had 2 components to the distribution, and the remaining 267 distributions did not clearly have 2 components, i.e. 68% of plasma sheet observations had multi-component ion distributions. Multi-component distributions were associated with $|\bar{B}| = 4.6$ nT, whereas for distributions where 2 populations could not be clearly identified, $|\bar{B}| = 3.4$ nT. Thus distributions are more likely to contain multiple populations at high rather than low field values. We also note that when considering the data ordered by individual crossings, 2 of the 33 crossings consisted entirely of multi-component populations, while 2 did not contain any clear evidence of multiple components.

Discussion and Conclusions

In the above case study, examples are provided of the high energy PSBL particles and multi-component outer plasma sheet distributions which appear to contain cold lobe-like plasma and outflowing heated lima-bean populations. We have also identified isotropic distributions and shell-like populations such as those outlined in *Owen and Mist* [2001] and *Hoshino et al.* [2000].

Our statistical survey of the distant tail data set shows that 68% of the 12 s distributions obtained during these rapid plasma sheet crossings contain two or more populations. During very rapid crossings, data may be aliased over

the 12 s period it takes to obtain the full 2D distribution. However, due to the number of crossings considered, we do not believe that this will have a significant effect on the overall results. In the distant tail, the PSBL is usually defined as being the region at the edge of the plasma sheet, where the field magnitude is close to but lower than in the lobe and there are some high energy, heated particles. We note that the distributions containing multi-component populations are clearly located within the distant tail plasma sheet and are not PSBL populations. If this were the case, we would expect a significantly higher magnetic field magnitude, much closer to the observed $|\overline{B}_L| = 11$ nT from this survey or, the previously reported $|\overline{B}_L| = 9.2$ nT [Slavin *et al.*, 1985] whereas $|\overline{B}_{PS}| = 4.6$ nT.

For the remaining 32% of the data set it was not possible to identify discrete populations. These observations are harder to classify. The particle population peak flux is below the detectors lower energy limit or the inflow and outflow populations may be close in velocity space and the combined distributions overlap. However, it is possible that the backscatter mechanism described in Owen and Mist [2001] could lead to particles being decelerated as well as accelerated and hence 'filling in' the distribution and leading to near-isotropic distributions. Within both classes of distribution, a component at higher energies than both the lobe and lobe populations was often observed. This component can be equated to the high-energy shell population modelled by Owen and Mist [2001]. These observations justify its inclusion in this model.

We find a difference in the average magnetic field magnitude associated with single (3.4 nT) and multi-component (4.6 nT) populations. This suggests the single component distributions are preferentially found near the centre of the plasma sheet, whereas multi-component distributions are found in the outer region. This result is consistent with those obtained in the Hoshino *et al.* [2000] case studies. However, our results show that even at the lowest field strength, where the spacecraft is assumed to be closest to the current sheet, ~ 50 % of distributions show clear evidence of multi-component plasmas. This is consistent with particle acceleration occurring at, or very close to, the cross tail current sheet, rather than at external slow mode shocks. The structure of the multi-component plasma sheet distributions can be understood in terms of the Owen and Mist [2001] current sheet acceleration model.

Acknowledgments. The Geotail MAG data were provided by the DARTS system at ISAS. RTM and CJO were

supported by PPARC, via a Post-Doctoral Research Assistantship and an Advanced Fellowship respectively.

References

- Cowley, S. W. H., Plasma populations in a simple open model magnetosphere, *Space Sci. Rev.*, **25**, 217, 1980.
- Hoshino, M., T. Mukai, I. Shinohara, and Y. Saito, Slow shock downstream structure in the magnetotail, *J. Geophys. Res.*, **105**, 337–347, 2000.
- Kokubun, S., T. Yamamoto, M. H. Acuña, K. Hayashi, K. Shiokawa, and H. Kawano, The GEOTAIL Magnetic Field Experiment, *J. Geomagn. Geoelectr.*, **46**, 7–21, 1994.
- Krauss-Varban, D., and N. Omidi, Large-scale hybrid simulations of the magnetotail during reconnection, *Geophys. Res. Lett.*, **22**, 3271, 1995.
- Lin, Y., and D. W. Swift, A two-dimensional hybrid simulation of the magnetotail reconnection layer, *J. Geophys. Res.*, **102**, 19859, 1996.
- Mukai, T., S. Machida, Y. Saito, M. Hirahara, T. Teresawa, N. Kaya, T. Obara, M. Ejiri, and A. Nishida, The Low Energy Particle (LEP) experiment onboard the GEOTAIL satellite, *J. Geomagn. Geoelectr.*, **46**, 669–692, 1994.
- Nagai, T., et al., Structure and dynamics of magnetic reconnection for substorm onsets with Geotail observations, *J. Geophys. Res.*, **103**, 4419–4440, 1998.
- Nishida, A., T. Mukai, T. Yamamoto, S. Kokubun, and K. Maezawa, A unified model of the magnetotail convection in geomagnetically quiet and active times, *J. Geophys. Res.*, **103**, 4409, 1998.
- Owen, C. J., and R. T. Mist, Distant plasma sheet ion distributions during reconnection, *Geophys. Res. Lett.*, **100**, 100, 2001.
- Owen, C. J., S. W. H. Cowley, and I. G. Richardson, Properties of the geotail plasma sheet - theory and observation, in *Magnetospheric Substorms*, *Geophys. Monogr. Ser.*, vol. 64, p. 215, AGU, Washington, D. C., 1991.
- Saito, Y., T. Mukai, T. Teresawa, A. Nishida, S. Machida, M. Hirahara, K. Maezawa, S. Kokubun, and T. Yamamoto, Slow-mode shocks in the magnetotail, *J. Geophys. Res.*, **100**, 23567, 1995.
- Slavin, J. A., E. J. Smith, D. G. Sibeck, D. N. Baker, R. D. Zwickl, and S. I. Akasofu, An ISEE 3 study of average and substorm conditions in the distant magnetotail, *J. Geophys. Res.*, **90**, 10,875, 1985.

R. T. Mist and C. J. Owen, Mullard Space Science Laboratory, Holmbury St. Mary, Surrey, RH5 6NT, England. (email: rtm@mssl.ucl.ac.uk; cjo@mssl.ucl.ac.uk)

Toshifumi Mukai, Institute of Space and Astronautical Science, 3-1-1 Yoshinodai, Sagami-hara, Kanagawa 229-8510, Japan. (email: mukai@stp.isas.ac.jp)

(Received February 12, 2001; revised June 19, 2001; accepted July 9, 2001.)